International Journal of Nanomedicine

Dovepress

open access to scientific and medical research

Open Access Full Text Article

ORIGINAL RESEARCH

^{131}I-Labeled Anti-HER2 Nanobody for Targeted Radionuclide Therapy of HER2-Positive Breast Cancer

Lingzhou Zhao*, Jiali Gong*, Qinli Qi*, Changcun Liu, Hongxing Su, Yan Xing, Jinhua Zhao

Department of Nuclear Medicine, Shanghai General Hospital, Shanghai Jiao Tong University School of Medicine, Shanghai, People's Republic of China

*These authors contributed equally to this work

Correspondence: Jinhua Zhao; Yan Xing, Department of Nuclear Medicine, Shanghai General Hospital, Shanghai Jiao Tong University School of Medicine, No. 100, Haining Road, Shanghai, 200080, People's Republic of China, Tel/Fax +86 21 3779 8352, Email zhaojinhua1963@126.com; xy.1@163.com

Purpose: The unique structure of nanobodies is advantageous for the development of radiopharmaceuticals for nuclear medicine. Nanobodies targeted to human epidermal growth factor receptor 2 (HER2) can be used as tools for the imaging and therapy of HER2-overexpressing tumors. In this study, we aimed to describe the generation of a ^{131}I-labeled anti-HER2 nanobody as a targeted radionuclide therapy (TRNT) agent for HER2-positive breast cancer.

Methods: The anti-HER2 nanobody NM-02 was labeled with ^{131}I using the iodogen method, and its radiochemical purity and stability in vitro were assessed. The pharmacokinetic profile of ^{131}I-NM-02 was investigated in normal mice. Tumor accumulation, biodistribution, and therapeutic potential of ^{131}I-NM-02 were evaluated in HER2-positive SKBR3 xenografts; HER2-negative MB-MDA-231 xenografts were used as the control group.

Results: ^{131}I-NM-02 could be readily prepared with satisfactory radiochemical purity and stability in vitro. Apparent tumor uptake was observed in HER2-positive tumor-bearing mice with rapid blood clearance and favorable biodistribution. ^{131}I-NM-02 could significantly inhibit tumor growth and extend the life of these mice with good organ compatibility. Negligible tumor accumulation and inhibitory effects of ^{131}I-NM-02 were observed in the negative control group.

Conclusion: ^{131}I-NM-02 has the potential to be explored as a novel tool for TRNT of HER2-positive breast cancer.

Keywords: human epidermal growth factor receptor 2, nanobody, ^{131}I, targeted radionuclide therapy

Introduction

Breast cancer is the most common cancer in women worldwide. It is classified into subtypes based on the expression levels of molecular biomarkers, including estrogen receptor, progesterone receptor, and human epidermal growth factor receptor 2 (HER2).[1–4] Approximately 20–30% of the patients with breast cancer have high HER2 expression.[5] HER2-overexpressing breast cancer is associated with more tumor aggressiveness, higher recurrence rate, and shorter overall survival. In recent years, HER2-targeted therapies have been the standard of care for patients with HER2-positive breast cancer.[6] Despite the effectiveness of this treatment, majority of the patients in this subset eventually progress due to acquired resistance.[7–9] Therefore, developing novel strategies that can enhance therapeutic efficacy or overcome drug resistance is of high importance.[10–12]

Targeted radionuclide therapy (TRNT) is a currently growing and potential strategy for cancer treatment.[13–15] In TRNT, therapeutic radionuclides accumulate in lesions of interest by physiologic uptake or by combining with carriers (such as antibodies, antibody fragments, peptides, and small molecules) that have high specificities and affinities with tumor cells.[15] Therefore, TRNT delivers specific irradiation to tumor lesions while sparing the surrounding healthy tissues. This makes TRNT an advantageous approach in the treatment of systemic malignancies when whole-body irradiation using external beam radiotherapy is intolerable due to severe toxicity. Over the past few decades, various

Received: 27 November 2022
Accepted: 4 April 2023
Published: 8 April 2023

radionuclides, including α particles (eg, ^{212}Pb, ^{227}Th), β particles (eg, ^{177}Lu, ^{131}I), and Auger electrons (eg, ^{111}In), have been used to develop TRNT agents for the treatment of HER2-positive breast cancer, such as ^{212}Pb-TCMC-trastuzumab, ^{227}Th-trastuzumab, ^{131}I-*N*-succinimidyl 4-guanidinomethyl-3-iodobenzoate (SGMIB)-anti-HER2 nanobody, ^{177}Lu-diethylenetriamine pentaacetate-2Rs15d nanobody, and ^{111}In-trastuzumab.[16–20]

Nanobodies, also referred to as single-domain antibodies, are small antigen-binding fragments mainly derived from *Camelidae* heavy-chain antibodies.[21–23] Owing to their low molecular weight (15 kDa) and complexity, nanobodies possess advantageous characteristics, such as good stability, high specificity, strong antigen-binding affinity, short circulation time, and deep tumor penetration, compared with conventional antibodies. These characteristics make them suitable for the development of TRNT agents. Various HER2-directed nanobodies have been successfully generated as vehicles for imaging and therapy approaches in breast cancer.[24–26] Multiple radionuclides have been labeled with HER2-directed nanobodies and evaluated as TRNT agents in preclinical studies.

We have recently reported the first-in-human SPECT/CT study of ^{99m}Tc-labeled anti-HER2 nanobody (^{99m}Tc-NM-02) for HER2 imaging in breast cancer.[27] The study showed that NM-02 had a high binding affinity to human HER2 antigen with a dissociation constant of 1.2 nM and had no competition with trastuzumab and pertuzumab for HER2 binding. SPECT/CT imaging showed obvious ^{99m}Tc-NM-02 accumulation in both primary and metastatic lesions in patients with high HER2 expression (HER2 2+ or 3+), whereas no distinct tumor uptake was observed in the representative HER2-negative patient (HER2 0), suggesting good specificity in vivo. Based on our previous findings, we aimed to further synthesize ^{131}I-labeled NM-02 and evaluate its potential as a TRNT agent for HER2-positive breast cancer.

Materials and Methods

Materials

Phosphate-buffered saline (PBS; pH 7.4), fetal bovine serum, Dulbecco's modified Eagle medium, iodogen (1,3,4,6-tetrachloro-3α,6α-diphenylglycoluril), and PD-10 desalting columns were obtained from Shanghai Dobio Co., Ltd. (Shanghai, China). NM-02 nanobodies and Na^{131}I solution were supplied by NanoMab (Shanghai, China) and Shanghai GMS Pharmaceutical Co., Ltd. (Shanghai, China), respectively. MDA-MB-231 (HER2-negative) and SKBR3 cells (HER2-positive) were obtained from Procell Life Science & Technology Co., Ltd. (Wuhan, China). All other chemicals and solvents were supplied by Sinopharm Chemical Reagent Co., Ltd. (Shanghai, China).

Preparation and Characterization of ^{131}I-NM-02

Prior to radiolabeling, 100 μL of iodogen in CH_2Cl_2 solution (1 mg/mL) was added to the bottom of a 10-mL centrifuge tube. The solvent was blow dried using nitrogen gas to form a thin solid layer on the tube wall. One hundred microliters of NM-02 solution (2 mg/mL, PBS, pH 7.4) was added to the bottom of the tube coated with iodogen, and then 100 μL of Na^{131}I (3.7 GBq/mL) was gently mixed. The mixture was then incubated at room temperature for 30 min with occasional shaking. Subsequently, the reaction mixture was purified via size-exclusion chromatography using a PD-10 desalting column with saline as the mobile phase.

The purified ^{131}I-NM-02 was characterized following a previously published protocol.[28] Briefly, analyses were performed using an Agilent 1260 high-performance liquid chromatography (HPLC) system (Agilent Technologies, Santa Clara, CA, USA) equipped with a UV-vis detector (λ = 280 nm) and a radioactive flow detector (BioScan, Houston, TX, USA). A BioSep SEC-s2000 column (5 μm, 145 Å, 300×7.8 mm; Phenomenex, Torrance, CA, USA) was used at a flow rate of 1 mL/min with the following method: 0.1% trifluoroacetic acid in H_2O and CH_3CN (0–30 min, 45% CH_3CN). The radiochemical purity (RCP) of ^{131}I-NM-02 was determined using HPLC and rapidly analyzed with instant thin-layer chromatography (ITLC) using a system consisting of ITLC–silica gel paper (Agilent) and citrate buffer (pH = 5.4) as the mobile phase. The ^{131}I-NM-02 was incubated in saline at room temperature to test its stability in vitro. RCPs within 24 h were evaluated using the ITLC method described above.

Cells and Animal Models

MDA-MB-231 and SKBR3 cells were cultured under conditions recommended by the supplier. Four-week-old female BALB/c nude mice (16–18 g) were purchased from Shanghai Laboratory Animal Center of the Chinese Academy of Sciences (Shanghai, China). Animal models were established according to previously published protocols.[29,30] Mice were subcutaneously injected in their right-side flanks with 150 μL of cell suspension, corresponding to 5×10^6 cells in a 1:1 PBS and Matrigel mixture. When the diameter of the tumor nodules reached 0.8–1.2 cm, the mice were used for animal experiments. Before animal experiments, the tumor-bearing mice were fed with water containing 1% potassium iodide (KI) for 3 days to block the thyroid uptake of ^{131}I-NM-02.

Pharmacokinetics of ^{131}I-NM-02

The pharmacokinetic profile of ^{131}I-NM-02 was studied in five 6-week-old normal ICR mice. Each mouse was administered 740 kBq ^{131}I-NM-02, corresponding to 1 μg of NM-02 in 200 μL of saline. Blood was collected in 10-μL capillary tubes at designated time points (1, 2, 5, 15, 30, 60, 90, and 120 min). The radioactivity of the blood samples was measured using a gamma counter (Capintec, Florham Park, NJ, USA) to calculate the percentage of injection dose per gram (% ID/g) of the wet tissue. Pharmacokinetic data were analyzed using DAS 2.0 (Shanghai, China), and the half-life of ^{131}I-NM-02 in the blood was analyzed using a three-compartment model.

SPECT Imaging and Biodistribution

SPECT imaging was performed to validate the accumulation of ^{131}I-NM-02 in HER2-positive tumors in vivo. Briefly, ^{131}I-NM-02 solution (200 μL, [^{131}I] = 370 MBq/mL, corresponding to 40 μg of NM-02) was intravenously injected into SKBR3 and MBA-MD-231 tumor-bearing mice. SPECT images were acquired 1, 2, 4, and 8 h after injection using an Infinia SPECT imaging system equipped with a Xeleris 2.0 workstation and high-energy general-purpose collimators (GE, Boston, MA, USA). Subsequently, all mice were immediately euthanized to harvest the tumors and major organs for ex vivo SPECT scans, and the biodistribution of ^{131}I-NM-02 at 8 h post-injection was determined.

Therapeutic Efficacy

The SKBR3 tumor-bearing mice established above were randomized into three groups (11 mice per group) and separately treated with ^{131}I-NM-02 (14.8 MBq, 200 μL, corresponding to 8 μg of NM-02), Na^{131}I solution (14.8 MBq, 200 μL), and saline (200 μL). For comparison, the same grouping and treatment were applied for MDA-MB -231 tumor-bearing mice. The treatment was conducted every 3 days for a total of five times. The tumor volume and body weight of each mouse were measured after each treatment. Three days after the end of the treatment, the representative mice from the groups were sacrificed to harvest the tumors and major organs (heart, liver, spleen, lung, and kidneys). Hematoxylin and eosin (H&E) and terminal deoxynucleotidyl transferase dUTP nick-end labeling (TUNEL) assays were performed according to standard protocols to investigate the therapeutic efficacy and biosafety of ^{131}I-NM-02 in vivo. The relative tumor volumes, body weights, and survival rates were calculated as described in our previous work.[31] Mice were euthanized when the tumor diameter exceeded 1.5 cm, body weight loss was more than 20%, or tumor ulceration occurred.

Statistical Analysis

Data are presented as mean ± standard deviation, and one-way analysis of variance was performed to evaluate the significance of the data using SPSS version 24.0 (IBM Corp., Armonk, NY, USA). A p-value of 0.05 was selected as the threshold of significance, and the levels of significant were as follows: *$p < 0.05$; **$p < 0.01$; ***$p < 0.001$.

Results

Preparation, Quality Control, and Stability of ^{131}I-NM-02

The production, purification, and characterization of NM-02 nanobodies bearing a hexahistidine tail have been previously described.[27] Briefly, the NM-02 nanobody was identified from a phage display library generated from *Camelus*

bactrianus immunized against human HER2 extracellular domain protein. Its equilibrium dissociation constant for binding to human HER2, determined using enzyme-linked immunosorbent assay, was 1.2 nM.

NM-02 was successfully radiolabeled with ^{131}I using the iodogen method. The characterization of ^{131}I-NM-02 was analyzed using HPLC and ITLC. As shown in Figure 1A, the HPLC result of ^{131}I-NM-02 showed a single radioactive peak with a retention time of 11.02 min, which was consistent with that of the corresponding NM-02 (10.63 min). The RCP of ^{131}I-NM-02 was calculated to be more than 99% without further purification. It can also be rapidly estimated using ITLC. ^{131}I-NM-02 displayed a retention factor of 0–0.2 (Figure 1B), and iodine ion and oxidized iodine had retention factors of 0.5–0.7 and 0.8–1.0, respectively.[32] Furthermore, the stability of ^{131}I-NM-02 was analyzed in PBS at room temperature via the ITLC method. ^{131}I-NM-02 was stable in PBS, with an RCP of greater than 95% up to 12 h, decreasing to 91% at 24 h (Figure 1C).

Pharmacokinetics of ^{131}I-NM-02

The radioactivity–time curve of ^{131}I-NM-02 between 1- and 240-min post-injection is shown in Figure 2. At 1 min post-injection, the radioactivity in blood was 14.99% ± 0.92% ID/g, which rapidly decreased to 4.32% ± 0.58% ID/g at 5 min

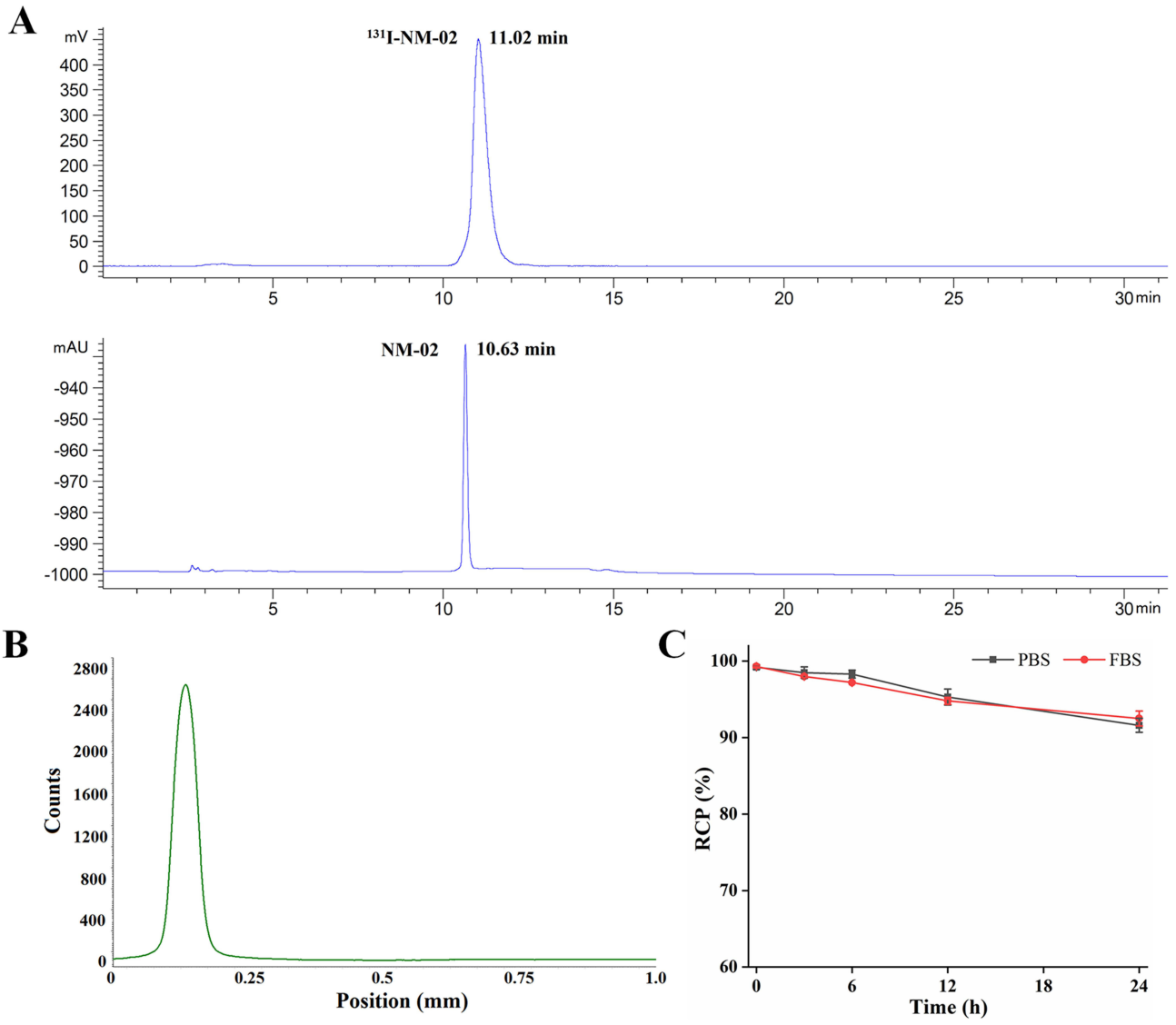

Figure 1 Characterization and stability of ^{131}I-NM-02. (**A**) HPLC and (**B**) ITLC results of ^{131}I-NM-02. (**C**) In vitro stability of ^{131}I-NM-02 in PBS at room temperature and fetal bovine serum at 37°C within 24 h.

Abbreviations: HPLC, high-performance liquid chromatography; ITLC, instant thin-layer chromatography; FBS, fetal bovine serum.

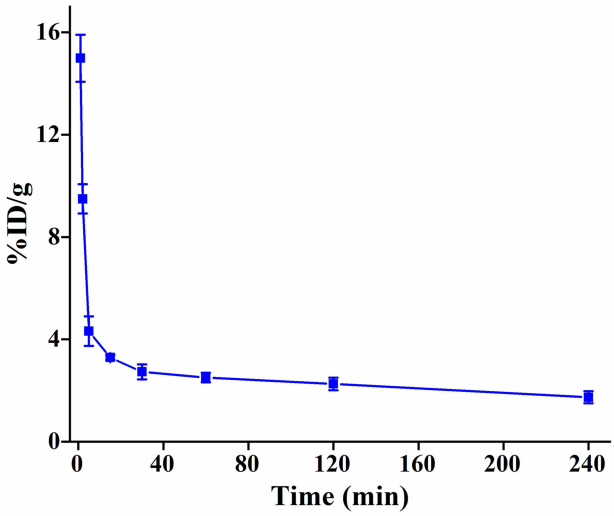

Figure 2 Pharmacokinetics of ^{131}I-NM-02. Blood clearance of ^{131}I-NM-02 in normal ICR mice.

post-injection. At 240 min post-injection, less than 2% ID/g could be recovered from the blood pool. To determine the biological blood half-life of ^{131}I-NM-02, a three-phase exponential fit was performed. The blood clearance was 0.07 L/min/kg, and the elimination half-life $t_{1/2\alpha}$, $t_{1/2\beta}$, and $t_{1/2\gamma}$ of ^{131}I-NM-02 were approximately 1.02, 11.71, and 69.32 min, respectively.

SPECT Imaging and Biodistribution

The schematic illustration of SPECT imaging is presented in Figure 3A. As shown in Figure 3B and C, a similar distribution pattern was observed in HER2-positive and HER2-negative tumor-bearing mice. ^{131}I-NM-02 mainly accumulated in the kidneys and urinary bladder, whereas other major organs, including the heart, lungs, liver, and muscle, had low uptake. Meanwhile, distinct tumor accumulation of ^{131}I-NM-02 was observed at 1 h post-injection and sustained over time in HER2-positive SKBR3 xenografts, whereas no obvious radioactivity accumulated in HER2-negative MBA-MD-231 tumors during the same time period. Tumor-to-muscle (T/M) SPECT signal ratios at different time points were measured to further compare the different tumor uptake (Figure 3D). In contrast to the stable T/M ratio in MBA-MD-231 tumor-bearing mice, the T/M ratio in HER2-positive SKBR3 xenografts continued to increase with time and was higher at each time point. This supports the target specificity of ^{131}I-NM-02 in vivo. After SPECT imaging, a biodistribution experiment was performed at 8 h post-injection to quantitatively analyze the radioactivity of the main organs and tumors from the SKBR3 and MBA-MD-231 tumor-bearing mice. Figure 3E shows major accumulation of radioactivity in the kidneys but relatively low accumulation in other organs. Higher tumor uptake was observed in HER2-positive SKBR3 xenografts, which was similar to the SPECT results. Moreover, HER2 expression levels in the tumors were confirmed by immunohistochemistry after SPECT imaging and muscle tissues were used as negative controls. As expected, high HER2 expression levels were found in SKBR3 tumors, whereas MBA-MD-231 tumors and muscle tissues showed low HER2 expression levels (Figure 4). This correlation further validates the specificity of ^{131}I-NM-02 for HER2 in vivo.

Therapeutic Efficacy

After treatment for 15 days, the relative tumor volume in HER2-positive SKBR3 xenografts followed the order of $Na^{131}I$ (9.84 ± 1.22 times) ≈ saline (9.60 ± 1.62 times) > ^{131}I-NM-02 (3.61 ± 0.36 times). Mice treated with saline and $Na^{131}I$ displayed exponential tumor growth with no significant difference, whereas a significant delay in tumor growth was observed in mice treated with ^{131}I-NM-02 (Figure 5A). Moreover, the antitumor efficacy of ^{131}I-NM-02 was supported by the longer survival rates of HER2-positive SKBR3 xenografts (Figure 5B). Half of the tumor-bearing mice treated with ^{131}I-NM-02 survived after 52 days, whereas all tumor-bearing mice treated with saline and $Na^{131}I$ were

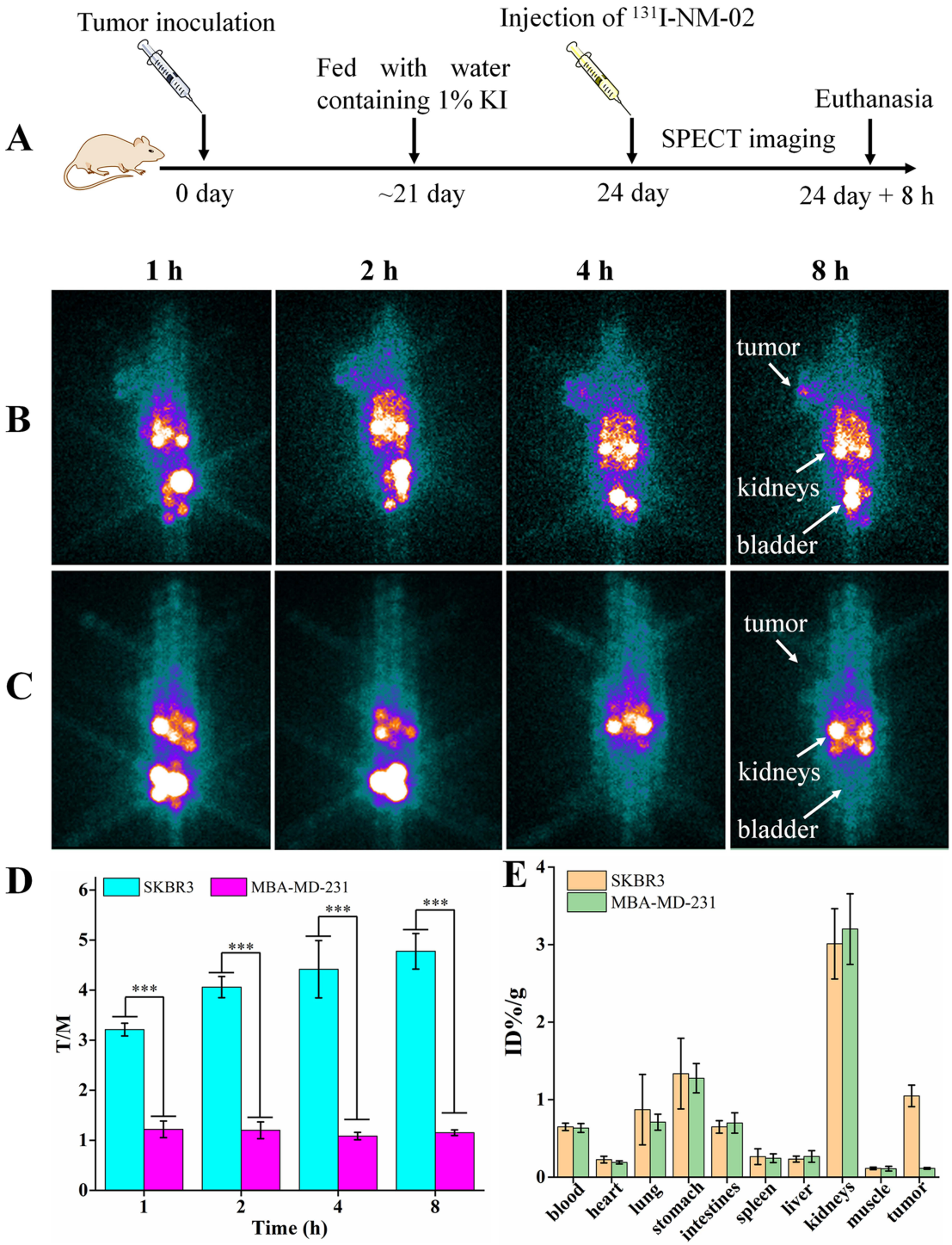

Figure 3 SPECT imaging and biodistribution of ^{131}I-NM-02. (**A**) Schematic illustration of SPECT imaging. SPECT images of (**B**) SKBR3 and (**C**) MBA-MD-231 tumor-bearing mice and (**D**) their T/M ratios at different time points after injection with ^{131}I-NM-02. (**E**) Biodistribution of ^{131}I-NM-02 in SKBR3 and MBA-MD-231 tumor-bearing mice at 8 h post-injection. Red arrows indicate tumors. The levels of significant were as follows:***$p < 0.001$.
Abbreviations: SPECT, single-photon emission computed tomography; T/M, tumor-to-muscle.

euthanized after 43 and 48 days, respectively. Furthermore, the body weight changes in mice in ^{131}I-NM-02 and Na^{131}I groups were similar to those in the saline group during treatment, and no notable difference was observed between them (Figure 5C), suggesting acceptable safety in vivo. H&E and TUNEL staining were performed to further evaluate the therapeutic effect of ^{131}I-NM-02. As shown in Figure 5D, H&E staining showed that apparent necrotic

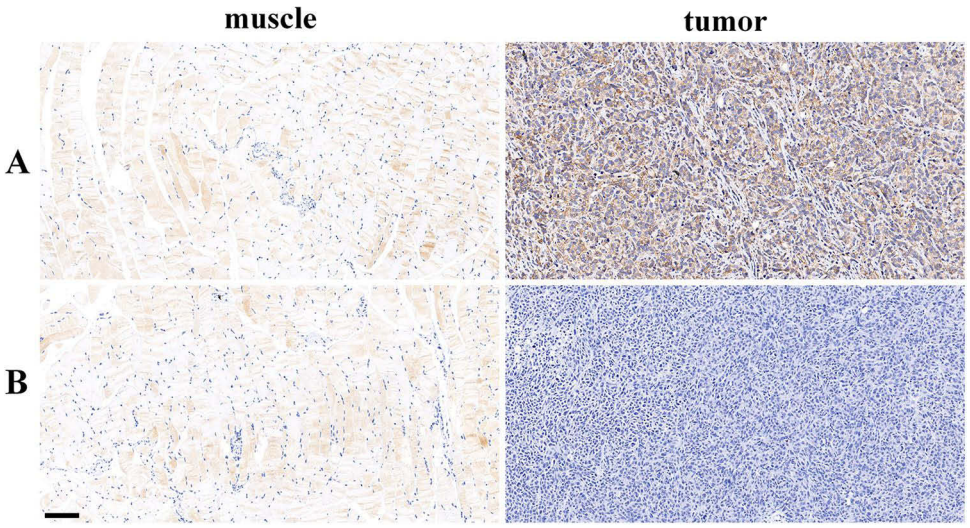

Figure 4 HER2 expression levels in the tumors. Immunohistochemistry images of HER2 in (**A**) SKBR3 and (**B**) MBA-MD-231 tumors and muscle (control). Scale bar represents 100 μm for both panels.

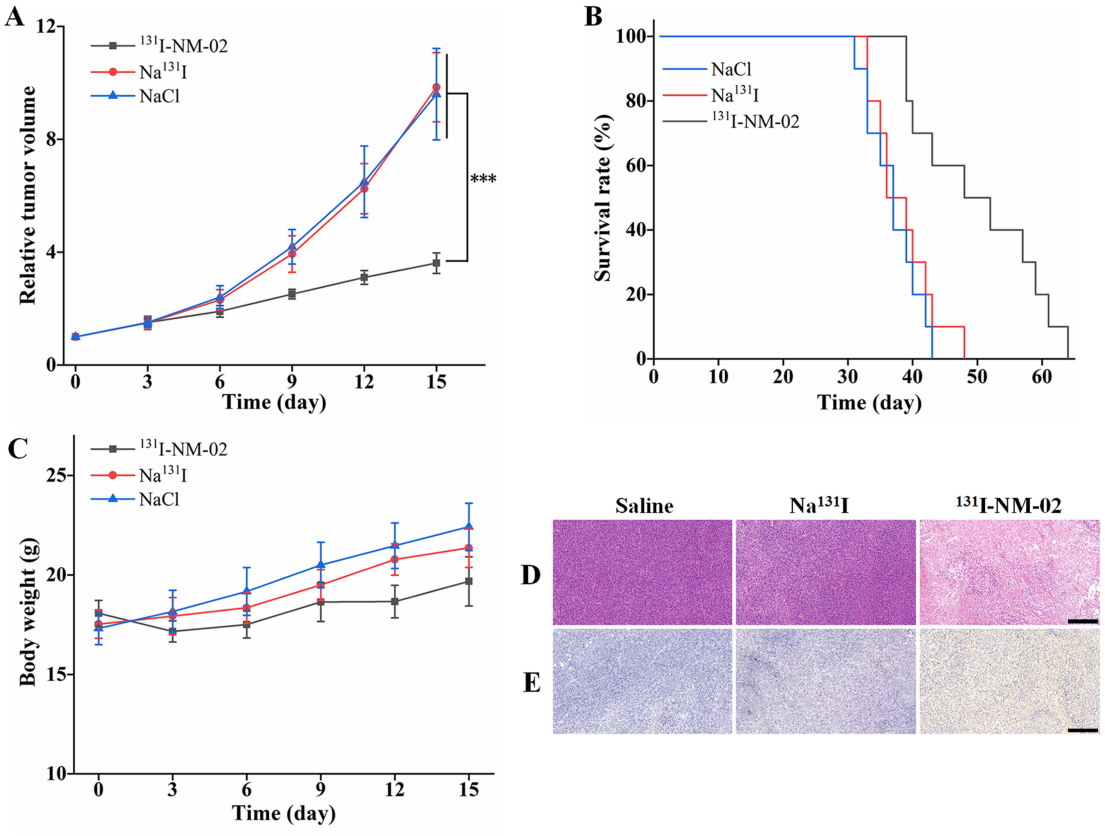

Figure 5 In vivo therapeutic efficacy of ^{131}I-NM-02 in HER2-positive tumors. (**A**) Relative tumor volume, (**B**) survival rate, (**C**) body weight, (**D**) H&E staining, and (**E**) TUNEL assay of SKBR3 xenografts after different treatments. Scale bar represents 200 μm for all panels. The levels of significant were as follows: ***$p < 0.001$.
Abbreviations: H&E, hematoxylin and eosin; TUNEL, terminal deoxynucleotidyl transferase dUTP nick-end labeling.

regions were only observed in HER2-positive SKBR3 xenografts treated with ^{131}I-NM-02. By contrast, well-shaped tumor cells and non-necrotic regions were observed after treatment with saline and Na^{131}I. Similarly, TUNEL staining revealed no apoptotic cells in the saline and Na^{131}I groups and displayed obvious positive staining of apoptotic cells,

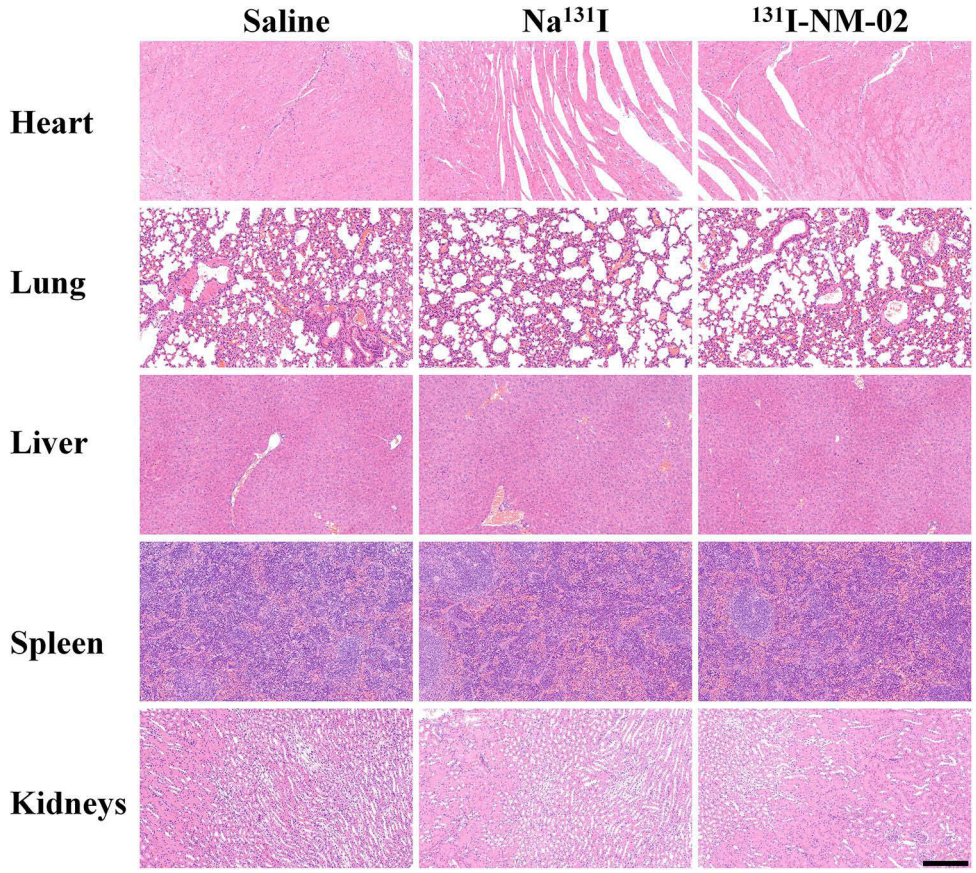

Figure 6 Biosafety of ^{131}I-NM-02. Representative H&E staining of major organs from SKBR3 xenografts after different treatments. Scale bar represents 200 μm for all panels.
Abbreviation: H&E, hematoxylin and eosin.

confirming antitumor performance in vivo (Figure 5E). HER2-negative MBA-MD-231 xenografts were used as controls. Unsurprisingly, the treatments using saline, Na^{131}I, and ^{131}I-NM-02 in HER2-negative MBA-MD-231 xenografts showed no significant differences in terms of tumor growth, survival rates, and body weight changes as well as H&E and TUNEL staining (Figure S1). Finally, the biosafety of ^{131}I-NM-02 was also investigated using H&E staining of the major organs (heart, liver, spleen, lung, and kidney) of the mice in all groups (Figures 6 and S2). No apparent organ damage or abnormalities were evidently observed, indicating that the developed ^{131}I-NM-02 had satisfactory organ compatibility.

Discussion

Approximately 20–30% of breast cancers demonstrate HER2 overexpression, which shows high aggressiveness, low sensitivity to endocrine therapy and chemoradiotherapy, and poor prognosis. Although HER2-targeted therapy has greatly improved the prognosis of patients with HER2-positive breast cancer, a considerable proportion of patients experience relapse and resistance to HER2-targeted drugs. Therefore, novel strategies for treating this malignant disease are of clinical importance.

TRNT has emerged as a promising strategy for cancer treatment. Nanobodies have attractive characteristics, including high specificity, strong antigen-binding affinity, short circulation time, and deep tumor penetration, for the development of TRNT agents. 2Rs15d was the first anti-HER2 nanobody to be applied as a TRNT agent for HER2-positive breast cancer treatment.[18] The tumor targeting, biodistribution, blood clearance, dosimetry, and safety of 2Rs15d were evaluated in preclinical and clinical studies after labeling with diagnostic radionuclides, including ^{18}F, ^{68}Ga, and ^{111}In.[33–35] Subsequently, ^{131}I-labeled 2Rs15d was generated, and its translational potential as a TRNT agent for HER2-overexpressing tumors was demonstrated in a preclinical study.[18] Subsequently, a Phase I trial of ^{131}I-labeled 2Rs15d showed a favorable toxicity profile and uptake in HER2-positive lesions, which further prompted a multicenter dose

escalation and therapeutic clinical investigation in patients with HER2-positive breast and gastric cancer.[36] The successful clinical translation of 2Rs15d motivated various attempts to develop more HER2-targeting TRNT agents for cancer therapy.

In our previous work, a library of anti-HER2 nanobodies was generated, and NM-02 was selected as the lead compound to develop molecular imaging tracers and TRNT agents for the diagnosis and treatment of HER2-positive cancers.[27] NM-02 showed high binding affinity (Kd = 1.2 nM), good in vivo tumor targeting, and noncompeting characteristic with trastuzumab and pertuzumab for HER2 targeting, which was validated preclinically after ^{99m}Tc radiolabeling. The ^{99m}Tc-labeled NM-02 showed good accumulation in the HER2-positive tumors at 90 min post-injection (8.37% ± 0.84% ID/g), and was further assessed in a first-in-human clinical trial, which found that it was safe for breast cancer imaging, with reasonable radiation doses, favorable biodistribution, and imaging characteristics. In the present study, we evaluated ^{131}I-labeled NM-02 as a TRNT agent for HER2-positive breast cancer therapy in tumor-xenografted mice. The main rationale for using ^{131}I in this study is its theranostic properties and the efficient radio-iodination of NM-02. The emission of β particles and γ rays allows ^{131}I to be used for radionuclide therapy and SPECT imaging. Currently, several methods are routinely used for iodine radiolabeling, including chloramine-T, iodogen, lactoperoxidase, and Bolton-Hunter. Moreover, SGMIB has been developed as a novel method for radioiodination. The better biodistribution and improved tumor uptake of biomolecules radioiodinated using SGMIB offer significant advantages over conventional iodination.[37] Even so, iodogen is a very convenient radiolabeling method for biomolecules due to the mild reaction condition, good repeatability, and less damage to biological activity. The presence of a hexahistidine tail and tyrosine residues in NM-02 resulted in effective radiolabeling of ^{131}I using the iodogen method.

We showed that the formed ^{131}I-labeled NM-02 had a high RCP and acceptable stability in vitro within 24 h. Nevertheless, the deiodination in vivo is a common occurrence. Therefore, mice were fed with water containing 1% KI for 3 days to block the thyroid uptake of ^{131}I before in vivo experiments. ^{131}I-NM-02 displayed good pharmacokinetics, and the fast blood clearance might be due to rapid extraction through the urinary system, which is similar to other radiolabeled nanobodies.[36] When injected intravenously into mice, ^{131}I-NM-02 is rapidly eliminated from the blood, which is beneficial for obtaining early diagnostic images with good contrast. Unsurprisingly, the HER2-positive tumors were visible as early as 1 h post-injection with sustained tumor accumulation of ^{131}I-NM-02 over time, whereas inconspicuous accumulation was observed in the HER2-negative tumors during the same time period. This result is consistent with the higher T/M ratio in HER2-positive SKBR3 xenografts than in the negative controls at each time point. The target specificity of ^{131}I-NM-02 to HER2-positive tumors in vivo was further supported by its higher tumor uptake in biodistribution experiments 8 h post-injection. The rapid blood clearance and high tumor accumulation of ^{131}I-NM-02 are in agreement with our previously obtained results from ^{99m}Tc-NM-02, revealing the potential for TRNT.[27]

The therapeutic efficacy of ^{131}I-NM-02 for HER2-positive tumors in vivo was demonstrated after five treatments. Mice with SKBR3 xenografts treated with ^{131}I-NM-02 showed significantly suppressed tumor growth and longer survival times than mice with HER2-negative tumors. After five treatments with ^{131}I-NM-02, the tumor volumes in HER2-positive and HER2-negative groups had increased 3.61 ± 0.36 and 11.12 ± 2.49 times, respectively. The evident tumor inhibition effect of ^{131}I-NM-02 is attributed to the enhanced tumor uptake via HER2-mediated targeting to breast cancer cells, which was also verified by longer survival. The survival time of mice with SKBR3 xenografts was extended up to 64 days after treatment with ^{131}I-NM-02, whereas all mice in the NaCl and Na^{131}I groups were euthanized at this time point. In addition, mice with SKBR3 or MDA-MB-231 xenografts that were treated with Na^{131}I or saline showed similar tumor growth and survival times to mice with MDA-MB-231 xenografts after ^{131}I-NM-02 treatment. No significant weight loss was observed in mice in each group, suggesting favorable in vivo safety of ^{131}I-NM-02. Furthermore, the therapeutic effect and safety in vivo of ^{131}I-NM-02 were confirmed using H&E and TUNEL assays. Necrotic regions were only found in mice treated with ^{131}I-NM-02, and the necrotic area in HER2-positive tumors was much larger than that in HER2-negative controls. Conversely, no apparent tumor cell necrosis was observed in mice treated with Na^{131}I or saline. Similarly, TUNEL staining revealed a large number of apoptotic cells in the SKBR3 tumors treated with ^{131}I-NM-02, but only a few or no apoptotic cells were detected in the tumors of other groups. In addition, H&E staining demonstrated no potential histological toxicity of ^{131}I-NM-02 in the major organs after five treatments. Taken together,

the results on the therapeutic effect and safety in vivo of ^{131}I-NM-02 indicate that the prepared ^{131}I-NM-02 has the potential to be used as a TRNT agent for HER2-positive breast cancer.

Conclusion

^{131}I-NM-02 could be readily prepared using the iodogen method with a high radiochemical yield and acceptable stability in vitro. The prepared ^{131}I-NM-02 displayed rapid blood clearance, favorable biodistribution, evident tumor accumulation, and significant therapeutic efficacy in HER2-positive tumor-bearing mice with good organ compatibility. Our data support the strong potential of ^{131}I-NM-02 as a TRNT agent for clinical translation.

Abbreviations

CT, computed tomography; H&E, hematoxylin and eosin; HPLC, high-performance liquid chromatography; HER2, human epidermal growth factor receptor 2; ITLC, instant thin-layer chromatography; SGMIB, N-succinimidyl 4-guanidinomethyl-3-iodobenzoate; RCP, radiochemical purity; SPECT, single-photon emission computed tomography; TRNT, targeted radionuclide therapy; TUNEL, terminal deoxynucleotidyl transferase dUTP nick-end labeling; T/M, tumor-to-muscle.

Ethics Approval

The animal experiments were approved by the Animal Ethics Committee of Shanghai General Hospital (no. 2022AW040), Shanghai Jiao Tong University School of Medicine, and conducted in accordance with the ethical standards of the National Health and Medical Research Council (China).

Acknowledgments

This research was supported by the Clinical Research Plan of the SHDC (SHDC2020CR2057B) and the National Natural Science Foundation of China (81971647 and 82171978).

Disclosure

The authors declare no potential conflicts of interest relevant to this article.

References

1. Sung H, Ferlay J, Siegel RL, et al. Global Cancer Statistics 2020: GLOBOCAN estimates of incidence and mortality worldwide for 36 cancers in 185 countries. *CA Cancer J Clin*. 2021;71(3):209–249. doi:10.3322/caac.21660
2. Xia C, Dong X, Li H, et al. Cancer statistics in China and United States, 2022: profiles, trends, and determinants. *Chin Med J*. 2022;135(5):584–590. doi:10.1097/cm9.0000000000002108
3. Prat A, Pineda E, Adamo B, et al. Clinical implications of the intrinsic molecular subtypes of breast cancer. *Breast*. 2015;24(Suppl 2):S26–S35. doi:10.1016/j.breast.2015.07.008
4. Loibl S, Poortmans P, Morrow M, Denkert C, Curigliano G. Breast cancer. *Lancet*. 2021;397(10286):1750–1769. doi:10.1016/S0140-6736(20)32381-3
5. Derakhshani A, Rezaei Z, Safarpour H, et al. Overcoming trastuzumab resistance in HER2-positive breast cancer using combination therapy. *J Cell Physiol*. 2020;235(4):3142–3156. doi:10.1002/jcp.29216
6. Oh D-Y, Bang Y-J. HER2-targeted therapies—a role beyond breast cancer. *Nat Rev Clin Oncol*. 2020;17(1):33–48. doi:10.1038/s41571-019-0268-3
7. Nahta R, Yu D, Hung M-C, Hortobagyi GN, Esteva FJ. Mechanisms of disease: understanding resistance to HER2-targeted therapy in human breast cancer. *Nat Clin Pract Oncol*. 2006;3(5):269–280. doi:10.1038/ncponc0509
8. Vernieri C, Milano M, Brambilla M, et al. Resistance mechanisms to anti-HER2 therapies in HER2-positive breast cancer: current knowledge, new research directions and therapeutic perspectives. *Crit Rev Oncol Hematol*. 2019;139:53–66. doi:10.1016/j.critrevonc.2019.05.001
9. Schlam I, Tarantino P, Tolaney SM. Overcoming resistance to HER2-directed therapies in breast cancer. *Cancers*. 2022;14(16):3996. doi:10.3390/cancers14163996
10. Díaz-Rodríguez E, Gandullo-Sánchez L, Ocaña A, Pandiella A. Novel ADCs and strategies to overcome resistance to anti-HER2 ADCs. *Cancers*. 2022;14(1):154. doi:10.3390/cancers14010154
11. Sidaway P. HER2-targeted agents overcome resistance. *Nat Rev Clin Oncol*. 2020;17(3):133. doi:10.1038/s41571-019-0325-y
12. Pernas S, Tolaney SM. HER2-positive breast cancer: new therapeutic frontiers and overcoming resistance. *Ther Adv Med Oncol*. 2019;11:1758835919833519. doi:10.1177/1758835919833519
13. Kleinendorst SC, Oosterwijk E, Bussink J, Westdorp H, Konijnenberg MW, Heskamp S. Combining targeted radionuclide therapy and immune checkpoint inhibition for cancer treatment. *Clin Cancer Res*. 2022;28(17):3652–3657. doi:10.1158/1078-0432.CCR-21-4332

14. Artigas C, Mileva M, Flamen P, Karfis I. Targeted radionuclide therapy: an emerging field in solid tumours. *Curr Opin Oncol*. 2021;33(5):493–499. doi:10.1097/cco.0000000000000762
15. Goldsmith SJ. Targeted radionuclide therapy: a historical and personal review. *Semin Nucl Med*. 2020;50(1):87–97. doi:10.1053/j.semnuclmed.2019.07.006
16. Meredith R, Torgue J, Shen S, et al. Dose escalation and dosimetry of first-in-human α radioimmunotherapy with ^{212}Pb-TCMC-trastuzumab. *J Nucl Med*. 2014;55(10):1636–1642. doi:10.2967/jnumed.114.143842
17. Abbas N, Heyerdahl H, Bruland SO, Brevik ME, Dahle J. Comparing high LET ^{227}Th- and Low LET ^{177}Lu-trastuzumab in mice with HER-2 positive SKBR-3 xenografts. *Curr Radiopharm*. 2013;6(2):78–86. doi:10.2174/18744710113069990017
18. D'Huyvetter M, De Vos J, Xavier C, et al. ^{131}I-labeled anti-HER2 camelid sdAb as a theranostic tool in cancer treatment. *Clin Cancer Res*. 2017;23(21):6616–6628. doi:10.1158/1078-0432.CCR-17-0310
19. D'Huyvetter M, Vincke C, Xavier C, et al. Targeted radionuclide therapy with a ^{177}Lu-labeled anti-HER2 nanobody. *Theranostics*. 2014;4(7):708–720. doi:10.7150/thno.8156
20. Keiko Li H, Hasegawa S. Favorable tumor uptake and nuclear transport of Auger electrons by nuclear targeting with ^{111}In-trastuzumab in an intraperitoneal tumor mouse model. *Nucl Med Commun*. 2022;43(7):763–769. doi:10.1097/mnm.0000000000001571
21. Liu M, Li L, Jin D, Liu Y. Nanobody-A versatile tool for cancer diagnosis and therapeutics. *Wiley Interdiscip Rev Nanomed Nanobiotechnol*. 2021;13(4):e1697. doi:10.1002/wnan.1697
22. Sun S, Ding Z, Yang X, et al. Nanobody: a small antibody with big implications for tumor therapeutic strategy. *Int J Nanomedicine*. 2021;16:2337–2356. doi:10.2147/IJN.S297631
23. Wang Y, Fan Z, Shao L, et al. Nanobody-derived nanobiotechnology tool kits for diverse biomedical and biotechnology applications. *Int J Nanomedicine*. 2016;11:3287–3303. doi:10.2147/IJN.S107194
24. Hrynchak I, Santos L, Falcão A, Gomes CM, Abrunhosa AJ. Nanobody-based theranostic agents for HER2-positive breast cancer: radiolabeling strategies. *Int J Mol Sci*. 2021;22(19):10745. doi:10.3390/ijms221910745
25. Altunay B, Morgenroth A, Beheshti M, et al. HER2-directed antibodies, affibodies and nanobodies as drug-delivery vehicles in breast cancer with a specific focus on radioimmunotherapy and radioimmunoimaging. *Eur J Nucl Med Mol Imaging*. 2021;48(5):1371–1389. doi:10.1007/s00259-020-05094-1
26. Li L, Liu T, Shi L, et al. HER2-targeted dual radiotracer approach with clinical potential for noninvasive imaging of trastuzumab-resistance caused by epitope masking. *Theranostics*. 2022;12(12):5551–5563. doi:10.7150/thno.74154
27. Zhao L, Liu C, Xing Y, et al. Development of a ^{99m}Tc-labeled single-domain antibody for SPECT/CT assessment of HER2 expression in breast cancer. *Mol Pharm*. 2021;18(9):3616–3622. doi:10.1021/acs.molpharmaceut.1c00569
28. Xing Y, Chand G, Liu C, et al. Early phase I study of a ^{99m}Tc-labeled anti–programmed death ligand-1 (PD-L1) single-domain antibody in SPECT/CT assessment of PD-L1 expression in non–small cell lung cancer. *J Nucl Med*. 2019;60(9):1213–1220. doi:10.2967/jnumed.118.224170
29. Rodallec A, Sicard G, Giacometti S, et al. Tumor uptake and associated greater efficacy of anti-Her2 immunoliposome does not rely on Her2 expression status: study of a docetaxel-trastuzumab immunoliposome on Her2+ breast cancer model (SKBR3). *Anticancer Drugs*. 2020;31(5):463–472. doi:10.1097/cad.0000000000000878
30. Zhang M, Guan Y, Zhong J, Chen X. Preparation and identification of HER2 radioactive ligands and imaging study of breast cancer-bearing nude mice. *Transl Oncol*. 2017;10(4):518–526. doi:10.1016/j.tranon.2017.04.003
31. Zhu J, Yang J, Zhao L, et al. ^{131}I-Labeled multifunctional polyethylenimine/doxorubicin complexes with pH-controlled cellular uptake property for enhanced SPECT imaging and chemo/radiotherapy of tumors. *Int J Nanomedicine*. 2021;16:5167–5183. doi:10.2147/IJN.S312238
32. Dong P, Cai H, Chen L, et al. Biodistribution and evaluation of ^{131}I-labeled neuropilin-binding peptide for targeted tumor imaging. *Contrast Media Mol Imaging*. 2016;11(6):467–474. doi:10.1002/cmmi.1708
33. Xavier C, Vaneycken I, D'huyvetter M, et al. Synthesis, preclinical validation, dosimetry, and toxicity of ^{68}Ga-NOTA-anti-HER2 nanobodies for iPET imaging of HER2 receptor expression in cancer. *J Nucl Med*. 2013;54(5):776–784. doi:10.2967/jnumed.112.111021
34. Xavier C, Blykers A, Vaneycken I, et al. ^{18}F-nanobody for PET imaging of HER2 overexpressing tumors. *Nucl Med Biol*. 2016;43(4):247–252. doi:10.1016/j.nucmedbio.2016.01.002
35. Massa S, Xavier C, De Vos J, et al. Site-specific labeling of cysteine-tagged camelid single-domain antibody-fragments for use in molecular imaging. *Bioconjug Chem*. 2014;25(5):979–988. doi:10.1021/bc500111t
36. D'Huyvetter M, Vos JD, Caveliers V, et al. Phase I trial of ^{131}I-GMIB-anti-HER2-VHH1, a new promising candidate for HER2-targeted radionuclide therapy in breast cancer patients. *J Nucl Med*. 2021;62(8):1097–1105. doi:10.2967/jnumed.120.255679
37. Pruszynski M, Koumarianou E, Vaidyanathan G, et al. Improved tumor targeting of anti-HER2 nanobody through N-succinimidyl 4-guanidinomethyl-3-iodobenzoate radiolabeling. *J Nucl Med*. 2014;55(4):650–656. doi:10.2967/jnumed.113.127100